

Two-dimensional distributed feedback lasers with thermally-nanoimprinted perylenediimide-containing films

EVA M. CALZADO,¹ ARITZ RETOLAZA,² SANTOS MERINO,² MARTA MORALES-VIDAL,^{3,4} PEDRO G. BOJ,⁵ JOSÉ A. QUINTANA,⁵ JOSÉ M. VILLALVILLA,³ AND MARÍA A. DÍAZ-GARCÍA^{3,*}

¹Dpto. Física, Ingeniería de Sistemas y Teoría de la Señal, and Instituto Universitario de Materiales de Alicante (IUMA), Universidad de Alicante, Alicante-03080, Spain

²Micro and Nano Fabrication Unit, IK4-Tekniker, Eibar 20600, Spain

³Dpto. Física Aplicada and IUMA, Universidad de Alicante, Alicante 03080, Spain

⁴Currently with Dpto. Física Aplicada, University of Salamanca, E-37008, Salamanca, Spain

⁵Dpto. Óptica and IUMA, Universidad de Alicante, Alicante 03080, Spain

*maria.diaz@ua.es

Abstract: Two-dimensional (2D) distributed feedback (DFB) lasers with gratings imprinted by thermal nanoimprint lithography on the active film are reported. They show thresholds for lasing of ~ 10 kW/cm², similar to the most efficient imprinted DFB lasers reported; and long operational lifetimes (under ambient conditions) of $\sim 12 \times 10^4$ pump pulses. The key for their successful operation has been the selection of a highly efficient and stable dye, perylene orange (PDI-O), and a proper matrix to host it, the fluoro-modified thermoplastic resist mr-I7030R, which has enabled 2D imprinting while preserving the dye optical properties. The use of the UV-curable resist SU8 as an alternative matrix for PDI-O to be imprinted by combined nanoimprint and photolithography was also investigated, and was concluded to be unsuccessful due to severe photoluminescence quenching. By replacing PDI-O with Rhodamine 6G, lasers with reasonable thresholds, but with significantly inferior operational lifetimes in comparison to PDI-O/mr-I7030R devices, were obtained.

©2017 Optical Society of America

OCIS codes: (220.4241) Nanostructure fabrication; (140.3490) Lasers, distributed-feedback.

References and links

1. C. Grivas, "Optically pumped planar waveguide lasers: Part II: Gain media, laser systems, and applications," *Prog. Quantum Electron.* **45–46**, 3–160 (2016).
2. A. J. Kuehne and M. C. Gather, "Organic lasers: recent developments on materials, device geometries, and fabrication techniques," *Chem. Rev.* **116**(21), 12823–12864 (2016).
3. E. Mele, A. Camposeo, R. Stabile, P. Del Carro, F. Di Benedetto, L. Persano, R. Cingolani, and D. Pisignano, "Polymeric distributed feedback laser by room-temperature nanoimprint lithography," *Appl. Phys. Lett.* **89**(13), 131109 (2006).
4. D. Pisignano, L. Persano, E. Mele, P. Visconti, M. Anni, G. Gigli, R. Cingolani, L. Favaretto, and G. Barbarella, "First-order imprinted organic distributed feedback lasers," *Synth. Met.* **153**(1-3), 237–240 (2005).
5. J. R. Lawrence, G. A. Turnbull, and I. D. W. Samuel, "Polymer laser fabricated by a simple micromolding process," *Appl. Phys. Lett.* **82**(23), 4023–4025 (2003).
6. G. L. Whitworth, S. Zhang, J. R. Y. Stevenson, B. Ebenhoch, I. D. W. Samuel, and G. A. Turnbull, "Solvent immersion nanoimprint lithography of fluorescent conjugated polymers," *Appl. Phys. Lett.* **107**(16), 163301 (2015).
7. M. G. Ramirez, P. G. Boj, V. Navarro-Fuster, I. Vragovic, J. M. Villalvilla, I. Alonso, V. Trabadelo, S. Merino, and M. A. Díaz-García, "Efficient organic distributed feedback lasers with imprinted active films," *Opt. Express* **19**(23), 22443–22454 (2011).
8. A. Retolaza, A. Juarros, D. Otaduy, S. Merino, V. Navarro-Fuster, M. G. Ramirez, P. G. Boj, J. A. Quintana, J. M. Villalvilla, and M. A. Díaz-García, "Thermal-nanoimprint lithography for perylenediimide-based distributed feedback laser fabrication," *Microelectron. Eng.* **114**, 52–56 (2014).
9. S. Riechel, C. Kallinger, U. Lemmer, J. Feldmann, A. Gombert, V. Wittwer, and U. Scherf, "A nearly diffraction limited surface emitting conjugated polymer laser utilizing a two-dimensional photonic band structure," *Appl. Phys. Lett.* **77**(15), 2310–2312 (2000).

10. E. B. Namdas, M. Tong, P. Ledochowitsch, S. R. Mednick, J. D. Yuen, D. Moses, and A. J. Heeger, "Low thresholds in polymer lasers on conductive substrates by distributed feedback nanoimprinting: progress toward electrically pumped plastic lasers," *Adv. Mater.* **21**(7), 799–802 (2009).
11. V. Reboud, P. Lovera, N. Kehagias, M. Zelsmann, C. Schuster, F. Reuther, G. Gruetzner, G. Redmond, and C. M. Sotomayor Torres, "Two-dimensional polymer photonic crystal band-edge lasers fabricated by nanoimprint lithography," *Appl. Phys. Lett.* **91**(15), 151101 (2007).
12. V. Reboud, J. Romero-Vivas, P. Lovera, N. Kehagias, T. Kehoe, G. Redmond, and C. M. Sotomayor Torres, "Lasing in nanoimprinted two-dimensional photonic crystal band-edge lasers," *Appl. Phys. Lett.* **102**(7), 073101 (2013).
13. S. Merino, H. Schiff, A. Retolaza, and T. Haatainen, "The use of automatic demolding in nanoimprint lithography processes," *Microelectron. Eng.* **84**(5-8), 958–962 (2007).
14. M. M. Jørgensen, S. R. Petersen, M. B. Christiansen, T. Buß, C. L. C. Smith, and A. Kristensen, "Influence of index contrast in two dimensional photonic crystals lasers," *Appl. Phys. Lett.* **96**(23), 231115 (2010).
15. M. B. Christiansen, T. Buß, C. L. C. Smith, S. R. Petersen, M. M. Jørgensen, and A. Kristensen, "Single mode dye-doped polymer photonic crystal lasers," *J. Micromech. Microeng.* **20**(11), 115025 (2010).
16. M. G. Ramírez, M. Morales-Vidal, V. Navarro-Fuster, P. G. Boj, J. A. Quintana, J. M. Villalvilla, A. Retolaza, S. Merino, and M. A. Díaz-García, "Improved performance of perylenediimide-based lasers," *J. Mater. Chem. C Mater. Opt. Electron. Devices* **1**(6), 1182–1191 (2013).
17. E. M. Calzado, J. M. Villalvilla, P. G. Boj, J. A. Quintana, V. Navarro-Fuster, A. Retolaza, S. Merino, and M. A. Díaz-García, "Influence of the excitation area on the thresholds of organic second-order distributed feedback lasers," *Appl. Phys. Lett.* **101**(22), 223303 (2012).
18. M. Imada, S. Noda, A. Chutinan, T. Tokuda, M. Murata, and G. Sasaki, "Coherent two-dimensional lasing action in surface-emitting laser with triangular-lattice photonic crystal structure," *Appl. Phys. Lett.* **75**(3), 316–318 (1999).
19. M. G. Ramírez, J. M. Villalvilla, J. A. Quintana, P. G. Boj, and M. A. Díaz-García, "Distributed feedback lasers based on dichromated poly(vinyl alcohol) reusable surface-relief gratings," *Opt. Mater. Express* **4**(4), 733–738 (2014).
20. M. Morales-Vidal, P. G. Boj, J. M. Villalvilla, J. A. Quintana, Q. Yan, N.-T. Lin, X. Zhu, N. Ruangsapichat, J. Casado, H. Tsuji, E. Nakamura, and M. A. Díaz-García, "Carbon-bridged oligo(*p*-phenylenevinylene)s for photostable and broadly tunable, solution-processable thin film organic lasers," *Nat. Commun.* **6**, 8458 (2015).

1. Introduction

Solution-processed planar waveguide organic lasers are inexpensive, integrable and mechanically flexible optoelectronic devices, with great potential in a variety of applications in the fields of spectroscopy, optical communications and sensing [1,2]. The distributed feedback (DFB) laser, consisting of a waveguide film which includes a relief grating, is a particularly interesting organic waveguide laser for various reasons: it requires low pump energy for operation, thus enabling pumping with compact and cheap sources; the resonator can be easily integrated into other devices; it can be mechanically flexible; has a potentially low production cost; and can be easily integrated with field-effect-transistor geometry, promising for the development of electrically-pumped organic lasers.

In most organic DFB lasers reported, the resonators have been fabricated over common inorganic transparent substrates (glass, SiO₂, etc.), by means of electron beam lithography (EBL), holographic lithography (HL), or nanoimprint lithography (NIL), followed by chemical or dry etching [1,2]. Resonator fabrication by directly engraving the active film by NIL is a very attractive approach for the purpose of obtaining flexible devices prepared in a simple way, thus with high potential to be scalable to mass production. A limitation shown by the organic DFB lasers with imprinted active films reported to date, is their relatively large thresholds (typically various tenths of kW/cm² and higher) [3–5] in comparison to state-of-the-art thresholds reported for DFB lasers based on highly efficient organic semiconductors and high quality resonators fabricated over inorganic substrates, often below 1 kW/cm² [1,2]. The generally high thresholds of devices with imprinted gratings are a consequence of the difficulty for many active materials to use thermal-NIL (T-NIL) (also called hot-embossing). T-NIL, based on the use of high pressure and temperature (typically above 100 °C), is the simplest and most standard technique used to imprint conventional thermoplastics, such as polystyrene (PS) or poly(methyl methacrylate), which provides very high fidelity pattern transfer and good aspect ratio. Unfortunately T-NIL cannot be used to imprint most active materials because their optical properties degrade upon the high temperatures used in the

procedures. So, alternative techniques such as room temperature NIL [3,4], solvent-assisted micro-contact molding [5], or solvent immersion imprint lithography [6] have been used, which in turn led to lower quality gratings and therefore a detrimental laser performance.

A breakthrough in the context of DFB lasers with gratings imprinted on the active film was the demonstration of one dimensional (1D) DFB lasers with imprinted films of PS doped with a perylenediimide (PDI) laser dye [7], which showed a threshold of only 8 kW/cm², among the lowest reported for imprinted organic DFB lasers; and simultaneously a very high operational durability (~10⁵ pump pulses, under excitation two times above threshold). Later on, 1D DFB devices based on PDIs dispersed in other thermoplastic polymers different than PS, were reported [8]. A key aspect for the success of these PDI-based imprinted devices was that the optical properties of the active materials were not affected by the T-NIL process to engrave the DFB gratings. This is a consequence of the use of certain PDIs, known for their excellent thermal, chemical and photostability; and well as the use of PS, very convenient from the processing point of view, for both film deposition and grating imprinting.

For 2D organic DFB lasers, as for 1D devices, the most common geometry consists in a surface-relief grating engraved on top of a substrate over which the organic active film is deposited [1,2,9]. There are few reports of 2D DFB lasers with gratings engraved on the active film by T-NIL [10–12]. As 2D structures want to be prepared, the selection of a proper resist becomes challenging because higher demolding forces are needed. Moreover, the facility of thermoplastic resists to deform and/or break in the demolding step process increases when surface roughness, surface contact or trapping of the polymer increase due to negative slopes of cavity sidewalls, being these aspects even more crucial when high aspect ratio structures are imprinted or when low molecular weight polymers are used [13]. A variation of T-NIL, which combines thermal and UV-curing to imprint a resist at a moderate low temperature, is the so-called combined nanoimprint and photolithography (CNP). CNP has been used to obtain 2D DFB lasers using pyrromethane as laser dye dispersed in UV-curable resists, such as Ormocore or SU-8 [14,15]. A drawback of CNP is that fewer resists are available, which constitutes a limitation to optimize properties such as the photostability.

In this work, T-NIL imprinted 2D DFB devices have been fabricated by using the fluoro-modified thermoplastic methacrylate-based resist mr-17030R doped with the N,N'-di(2,6-diisopropylphenyl)perylene-3,4:9,10-tetracarboxylicdiimide dye, known as perylene orange (PDI-O). The motivation to use PDI-O is to benefit from its high photoluminescence (PL) efficiency, excellent thermal, chemical and photostability and good performance as laser dye [7,8,16]. A key aspect is to find a proper matrix for PDI-O, so the material shows simultaneously a high performance as active laser media, a good capacity to be processed as a waveguide and to be imprinted with 2D relief gratings of sufficient quality. The possibility of using a CNP process with the SU8 resist, serving as host for the PDI-O, as well as for Rhodamine 6G (Rh6G), has also been investigated.

2. Experimental techniques

DFB devices were fabricated by either T-NIL or CNP (Fig. 1). The T-NIL process (Fig. 1(a)), consisted of the following steps: i) 270 nm and 500 nm-thick films of fluoro-modified mr-17030R resist (Micro Resist Technology GmbH) doped with 1 wt% of PDI-O ($M_w = 711$ g/mol, purity > 99.5%; supplied by Phiton) were spin-coated over a silicon oxide (SiO₂) layer grown over a silicon wafer; ii) the dye-doped resist was imprinted at 135 °C under vacuum, by applying a pressure of 20 bars for 15 min; and iii) manual demolding was performed at 40 °C. CNP fabrication (Fig. 1(b)) was performed as follows: i) a 650 nm-thick SU-8 2000.5 negative resist (MicroChem Corporation) film doped with 0.4 wt% of Rh6G ($M_w = 464,98$ g/mol, purity > 95%; Exciton Inc.) was spin-coated over a SiO₂ wafer; ii) a pressure of 15 bars was applied for 10 min in vacuum at 90 °C; iii) the master/substrate stack was UV flood exposed and post exposure baked in a EVG620 UV aligner: 11 cycles of 21 s of UV exposure at 10 mW/cm², followed by 15 s breaks for cooling; iv) the master was manually demolded;

and v) the substrate was developed. For both, T-NIL and CNP, a transparent fused silica stamp, fabricated by EBL and reactive ion etching, including 2D gratings with periodicities of 190 nm and 350 nm and a depth of 100 nm, over an area of $(2.5 \times 2.5) \text{ mm}^2$, was used. The master was subsequently treated with a fluorosilane coating, deposited from the vapor phase, to facilitate the demolding. DFB morphological characterization was performed by optical microscopy (AXIO Imager.A1m, Carl Zeiss), field emission scanning electron microscopy (FE-SEM, ZEISS Ultra Plus) and atomic force microscopy (AFM, NT-MDT Solver PRO). Film thickness was measured with a Dektak 8 surface profiler.

Optical DFB characterization was performed under excitation with a pulsed Nd:YAG (YAG-yttrium aluminum garnet) laser (10 ns, 10 Hz) operating at 532 nm [7,16,17]. The pump beam (incident at a 20° angle with respect to the normal to the film plane), was elliptical with a minor axis of 1.1 mm. The emitted light was collected with an Ocean Optics MAYA fiber spectrometer (resolution of 0.13 nm) in a direction perpendicular to the sample surface. The PL and amplified spontaneous emission (ASE) properties of the films, prior to grating imprinting, were also measured. For PL, a Jasco FP-6500 fluorimeter was used. ASE characterization was performed with the same excitation source used for DFB measurements. The pump beam was shaped to a stripe of dimensions $(3 \times 0.5) \text{ mm}^2$ and the emission collection was done from the edge of the film at the end of the stripe with an Ocean Optics USB2000 fiber spectrometer (resolution of 1.3 nm) [17].

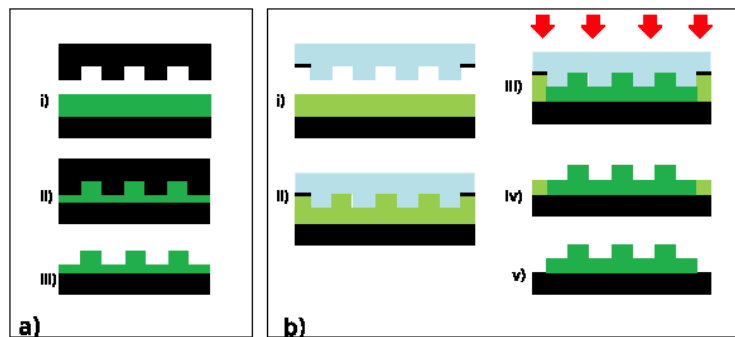


Fig. 1. Nanofabrication techniques: (a) T-NIL, i) spin-coating, ii) imprint, iii) demolding; and (b) CNP, i) spin-coating, ii) imprint, iii) UV exposure, iv) demolding and v) development.

3. Results and discussion

3.1 PL and ASE spectra of films without gratings

The potential of the resists mr-I7030R and SU8 to host the PDI-O dye was first investigated through their PL properties. Figure 2(a) shows the PL spectra for films of both resists without imprinted gratings doped with 1 wt% of PDI-O. For comparison purposes, data for a PS film doped with the same PDI-O content has also been included, because PS has been the matrix used with this and other PDIs in previous studies about 1D DFB lasers [7,16,17]. We chose this dye concentration because it showed the best performance, i.e. combination of lowest threshold and highest photostability [16]. It is seen that film PL intensity is highly dependent on the matrix: with mr-I7030R, significant PL intensity is obtained, although it is around four times smaller than the value obtained with PS; whilst with SU8, the PL emission is practically quenched, indicating that this matrix cannot be used with PDI-O.

As expected from the PL results, ASE was observed only in the PDI-O-doped mr-I7030R film, but not in the one based on SU8. The ASE spectrum of the mr-I7030R film (shown also in Fig. 2(a)) is similar to that obtained with PS [16]: it appears at $\lambda = 581 \text{ nm}$, close to the first vibronic PL peak, and has a linewidth (defined as the full width at half of its maximum, FWHM) of 4.3 nm. The ASE threshold, determined from a plot of the FWHM versus the pump intensity, as the pump intensity at which the linewidth decreases to half of its maximum

value, is 20 kW/cm^2 . This value is several times higher than the one obtained in PS (3 kW/cm^2) [16] and is attributed to the lower PL efficiency of PDI-O in this matrix. The ASE photostability half-life (number of pump pulses or time at which the ASE intensity decays to half of its initial value) in ambient conditions, is 1.5×10^4 pump pulses (25 min) under excitation at 40 kW/cm^2 (two times above threshold). This value is significantly inferior to that obtained with PS (3×10^5 pump pulses, under excitation at 6 kW/cm^2 , i.e. two times above its threshold), mainly because the threshold is higher, so the film needs to be pumped stronger. Nevertheless, the important result here is that the obtained ASE parameters are still reasonably good as to progress forward into the fabrication of 2D DFB lasers. It should be noted that our attempt to fabricate 2D DFB devices with T-NIL using PS as a host for PDI-O, as an obvious extension of our previous work with 1D devices, has not been successful due to problems in the demolding step.

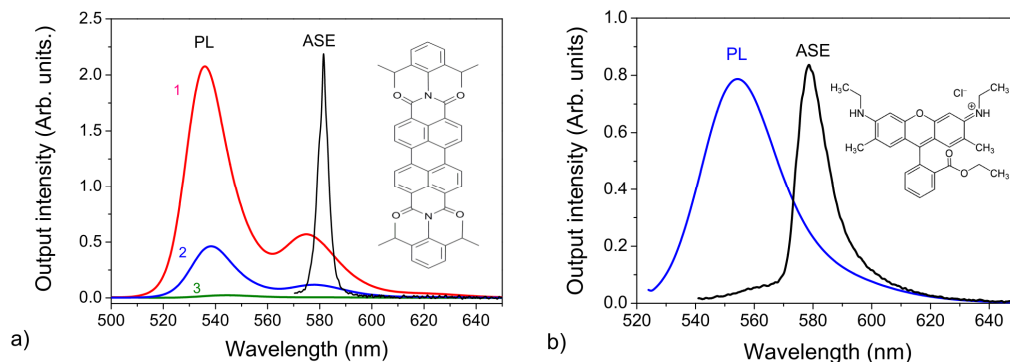


Fig. 2. (a) Normalized PL spectra (i.e. PL intensity divided by film thickness) of 1 wt%- PDI-O-doped films of PS, mr-I7030R and SU-8 (1 red, 2 blue and 3 green curves, respectively); and ASE spectrum for the mr-I7030R film (black curve); (b) PL and ASE spectra (blue and black lines, respectively) of SU8 doped with 0.4 wt% of Rh6G.

In the case of SU8, since PDI-O shows severe PL quenching in this matrix, we tried Rh6G as an alternative dye. Films with Rh6G concentrations ranging from 0.1 to 3 wt% were prepared and their PL and ASE properties characterized (see data for the film with 0.4 wt% in Fig. 2(b)). A decrease in threshold with increasing dye concentration was observed up to 0.4 wt%, at which the threshold reached a minimum value (4.5 kW/cm^2). Then, it started increasing up to 8 and 12 kW/cm^2 , for the films with 2 and 3 wt% respectively, presumably due to aggregation-induced PL quenching. With regards to the photostability performance, the ASE half-life of the 0.4 wt%-doped film, under excitation two times above threshold (i.e. 9 kW/cm^2) was 3×10^3 pump pulses (5 min). This value is significantly lower than that obtained with PDI-O dispersed in mr-I7030R, despite the smaller pump intensity used.

3.2 2D DFB lasers with PDI-O/mr-I7030R and Rh6G/SU8 active films

Two 2D DFB lasers with T-NIL imprinted films of PDI-O-doped mr-I7030R with thickness 270 nm and 500 nm were fabricated (devices labelled as I and II, respectively). Their laser spectra (Fig. 3(a)) show two narrow peaks (linewidths $\sim 0.5 \text{ nm}$), located at wavelengths of 560.5 and 563.1 nm (for device I) and at 575.7 and 577.2 nm (for device II). The separation between the two peaks is consistent with the two expected peaks at each side of the band gap [14,15,18]. The different emission wavelengths of devices I and II are a consequence of their different film thickness. Remarkably, a DFB threshold (Fig. 3(b)) of only 10 kW/cm^2 was obtained for device II, which is among the lowest reported for DFB devices with gratings imprinted by NIL directly on the active film [10–12]. This threshold is significantly lower than that of device I (around 200 kW/cm^2), firstly because device II has a thicker film, which implies a higher film absorption, PL efficiency and a better confinement of the waveguide mode; and secondly, because device II emits closer to the wavelength of maximum gain (i.e.

that at which ASE occurs, $\lambda_{\text{ASE}} = 581 \text{ nm}$ [19,20]. The DFB photostability half-life for device II is 1.7×10^4 pump pulses (28.3 min) under excitation at two times above threshold.

A 2D DFB laser based on Rh6G-doped SU-8 was also prepared (device III), in this case by means of CNP. The laser spectrum showed two peaks, at 591.1 and 592.4 nm, and its threshold was around 30 kW/cm^2 (see Figs. 3(a) and 3(b)) This value is somewhat larger than that obtained in device II, in spite of the lower ASE threshold, as discussed in section 3.1. This is attributed to the fact that laser emission occurs farther away from λ_{ASE} , which could be easily changed by further adjustment of the grating parameters and active film thickness. A photostability half-life of 4.3×10^3 pump pulses (7.2 min) was measured for device III, under excitation at two times above threshold in ambient conditions. In agreement with the ASE observations, this indicates that the photostability of this material is significantly inferior to that of PDI-O-doped mr-I7030R. In previous works of 2D DFB lasers based on the Rh6G dye, fabricated by either NIL or CNP, the photostability performance was also rather poor. For example in Ref [12], an operational half-life value of only 2×10^3 pump pulses, measured in vacuum, was reported. From the point of view of quality grating, for both types of processing, T-NIL or CNP, good fidelity pattern transfer was obtained (see Figs. 3(c) and 3(d)): grating periods and depth were the same as those of the master stamp.

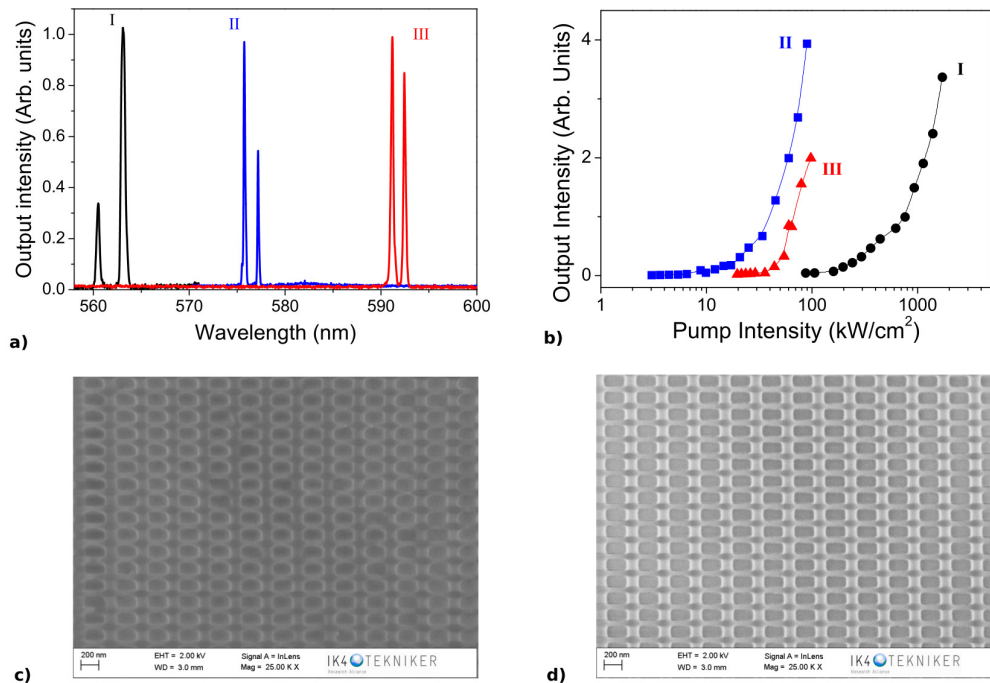


Fig. 3. (a) Spectra and (b) output versus pump intensity curves for various 2D DFB lasers: devices I and II, with T-NIL imprinted gratings on 270 and 500 nm-thick PDI-O/mr-I7030R active films, respectively; device III: with a CNP imprinted grating on a 650 nm-thick Rh6G/SU8 film; (c) and (d) SEM images for devices II and III, respectively.

4. Summary and conclusions

We have fabricated T-NIL imprinted 2D DFB devices by using perylene orange (PDI-O) dispersed in the fluoro-modified thermoplastic resist mr-I7030R showing thresholds for lasing of $\sim 10 \text{ kW/cm}^2$ and operational lifetimes of $\sim 2 \times 10^4$ pump pulses in ambient conditions. The good performance shown is a consequence of the proper selection of dye and matrix. Remarkably, the high PL efficiency and stability of the dye are preserved after grating

fabrication. We also found that the use of a CNP process with the PDI-O dye dispersed in the SU8 resist was not possible because of severe quenching of the PDI-O PL emission. Alternatively, for these SU-8 devices, the use of other dyes such as Rh6G has allowed to obtain lasers with reasonable thresholds ($\sim 30 \text{ kW/cm}^2$) but operational lifetimes ($\sim 4 \times 10^3$ pump pulses) significantly inferior than those of the PDI/mr-I7030R systems.

Funding

We thank support from the Spanish Government (MINECO) and the European Community (FEDER) through Grants MAT2011-28167-C02 and MAT2015-66586-R, as well as to the University of Alicante. M.M-V. has been partly supported by a MINECO FPI fellowship (no. BES-2009-020747) and by a Junta de Castilla y León grant (no. SA046U16).